Self-Stabilized Heterometallic Pair Sites for Selective Ethanol Dehydrogenation on Pt–Cr–Ag Alloy Catalysts

Jason F. Weaver,[a,*] Shuting Xiang,[b] Jovenal Jamir,[a] Ulrike Küst,[c] Lisa Rämisch,[d] Andrea Grespi,[c] Harald Wallander,[e] Johan Zetterberg,[d] Steven Arias,[f] Esteban L. Fornero,[g] Prahlad K. Routh,[b] Shengjie Zhang,[h] John S. Miller,[i] Rajeev Kumar Rai,[j] Eric A. Stach,[j] J. Anibal Boscoboinik,[f] Matthew M. Montemore,[h] E. Charles H. Sykes,[k,l] Jan Knudsen,[c,m] Jürgen Biener,[i,*] Lindsay R. Merte,[e,*] Anatoly I. Frenkel [b, n,*]

[a]Department of Chemical Engineering, University of Florida; Gainesville, FL 32611 USA.
[b]Department of Materials Science and Chemical Engineering, Stony Brook University; Stony Brook, NY 11794, USA.
[c]Division of Synchrotron Radiation Research and NanoLund, Department of Physics, Lund University, SE-22100 Lund, Sweden.
[d]Division of Combustion Physics, Lund University; Box 118, SE-221 00 Lund, Sweden.
[e]Department of Materials Science and Applied Mathematics, Malmö University; 20506 Malmö, Sweden.
[f]Center for Functional Nanomaterials, Brookhaven National Laboratory; Upton, New York 11973, USA.
[g]Instituto de Desarrollo Tecnológico para la Industria Química, Universidad Nacional del Litoral (UNL) y CONICET; Güemes 3450, 3000 Santa Fe, Argentina.
[h]Department of Chemical and Biomolecular Engineering, Tulane University; New Orleans, LA 70118 USA.
[i]Materials Science Division, Physical and Life Sciences Directorate, Lawrence Livermore National Laboratory; 7000 East Ave., Livermore, CA, 94550, USA.
[j]Department of Materials Science and Engineering, University of Pennsylvania, Philadelphia, PA 19104, USA
[k]Department of Chemistry, Tufts University; Medford, MA 02155, USA.
[l]Department of Chemical and Biological Engineering, Tufts University; Medford, MA 02155, USA.
[m]MAXIV Laboratory, Lund University, SE-22100 Lund, Sweden
[n]Division of Chemistry, Brookhaven National Laboratory; Upton, NY 11973, USA.

*Corresponding author. Email: weaver@che.ufl.edu (J.F.W.); biener2@llnl.gov (J.B.); lindsay.merte@mau.se (L.R.M.); anatoly.frenkel@stonybrook.edu (A.I.F.)

Abstract: Self-stabilized, heterometallic pair-sites can enable fine-tuning of catalytic functionality while also mitigating dynamic structural changes that degrade catalytic performance. This study demonstrates the development and characterization of trimetallic $Pt_xCr_xAg_{1-2x}$ ($x \leq 0.1$) alloys with active Pt-Cr pair-ensembles for non-oxidative ethanol dehydrogenation, leveraging predictions that favorable bonding stabilizes Pt-Cr pairs diluted in Ag. Operando X-ray absorption spectroscopy confirms the preferential formation and stability of Pt-Cr pairings dispersed throughout the Ag matrix, and ambient-pressure X-ray photoelectron spectroscopy shows that Pt-Cr sites have significant activity for ethanol dehydrogenation, while suppressing reaction processes that deactivate binary Pt-Ag and Cr-Ag alloys. This work demonstrates that stabilizing heterometallic pair sites within trimetallic alloys provides a new avenue for designing catalysts with discrete active sites that are durable and highly selective.

Introduction

Single-site catalysts can achieve high selectivity by providing atomically dispersed and uniform active sites, but stabilizing these materials under reaction conditions remains a challenge for their use in practical applications. In single-atom alloy (SAA) catalysts [1], a sub-class of single-site catalysts [2-3], the active sites are isolated atoms of a reactive metal dispersed throughout a less reactive host metal. SAA catalysts can achieve high selectivity largely because the low nuclearity of the active sites prevents multiple-step reactions toward undesirable products. However, adsorbed intermediates can induce segregation and aggregation of the active metal, leading to a loss of selectivity [4-10]. To reduce the risk of restructuring and degradation in performance, SAA catalysts are typically synthesized with low loadings (< 1%) of the active metal, thereby sacrificing catalytic activity for selectivity.

Compared with SAAs, dual-atom alloys (DAAs) offer broader opportunities for selective chemical transformations, including multistep chemical reactions, while providing greater stability of the active sites. Catalysts with atomically dispersed pair-sites or pair-ensembles have potential to expand the scope of discrete-site catalysts; however, their development has been limited by difficulty in stabilizing these active sites [11-16]. In a DAA, two reactive metals (A-B), present in minority concentrations, preferentially bond with one another and disperse throughout a less reactive host (C), generating chemically reactive, heterometallic dimers [17]. These heterometallic pair-sites can promote chemistries that single-atom sites cannot because they are larger and composed of metal atoms with different chemical functionalities. Furthermore, the favorable bonding that stabilizes the heterometallic pairs can improve their resistance toward restructuring in reactive environments. This stability stems from the preferential hetero-pairing of the reactive metals, analogous to the bonding in intermetallic compounds [18-19]. However, unlike traditional intermetallics, dual-atom alloys can preserve the discrete and isolated nature of their active sites. This combination of properties could allow dual-atom alloy catalysts to stabilize higher concentrations of active sites compared to SAAs and other pair-site catalysts, thereby enhancing both catalytic activity and selectivity.

Calculations using density functional theory (DFT) recently identified the PtCr-Ag(111) surface as a promising DAA for experimental studies, predicting not only that Pt-Cr pair-sites are energetically preferred in Ag(111) but also that they can promote the dehydrogenation of ethanol (CH_3CH_2OH) to acetaldehyde (CH_3CHO) under mild reaction conditions [20]. The Pt and Cr atoms provide distinct chemical functionalities [21] that, when combined, provide a facile pathway for the selective dehydrogenation of ethanol to acetaldehyde and H_2, which is a reaction of significant technological interest [22]. Experiments performed in ultrahigh vacuum confirmed the above mentioned DFT predictions [20], demonstrating that first-principles calculations can successfully guide the design of a DAA surface with distinct chemical properties compared with their SAA counterparts. Although computational studies suggest that DAAs with various hosts, including Cu, Ag and Au, and dopants can provide high performance for several important reactions [17, 23-27], experimental studies of DAAs and dilute trimetallics remain sparse [20, 28-29]. In particular, probing heterodopant interactions in dilute trimetallics under reaction conditions is challenging yet crucial for establishing the nature of the active site.

Herein we report the successful synthesis of Cr_xAg_{1-x}, Pt_xAg_{1-x}, and $Pt_xCr_xAg_{1-2x}$ alloy thin-films via controlled sputter-deposition. Catalytic testing demonstrated that the trimetallics are active, selective, and stable for the ethanol dehydrogenation reaction under practical conditions, whereas the bimetallic Pt-Ag and Cr-Ag systems are not. Despite their structural complexity, we demonstrate how bulk- and surface-sensitive X-ray spectroscopies can characterize their structure and dynamic segregation under reactive atmospheres and quantify the Pt-Cr pairings responsible for the reactivity. Significantly, *operando* X-ray spectroscopy reveals that preferential Pt-Cr pairing intrinsically stabilizes the active sites on Pt-Cr-Ag surfaces, ensuring sustained catalytic performance at high active-metal loadings.

Thin films (100 nm and 5 μm in thickness) of bimetallic Pt_xAg_{1-x} and Cr_xAg_{1-x} and trimetallic $Pt_xCr_xAg_{1-2x}$ alloys of various compositions (x = 0.02, 0.05 and 0.1) were magnetron sputter-deposited onto polycrystalline Ag (poly-Ag) and glass substrates (Supporting Information - SI). Scanning transmission electron microscopy (STEM) shows that the alloy films have a columnar grain structure with a characteristic grain width of several hundred nm (Fig. 1A). The films are characterized by a high density of stacking faults and stacking tetrahedra, which produce bright contrast in STEM images obtained at longer camera

length (CL) due to strain-induced contrast variations (Fig. 1A,B) but not at lower CL where Z-dependent contrast dominates in comparison to the smaller effects due to electron channeling caused by strain, stacking faults and stacking tetrahedron defects (Fig. 1C) [30-31]. The absence of abrupt contrast variations in higher resolution images at lower CL demonstrates that Pt or Cr clustering occurs negligibly at length scales of ~1 nm (Fig. 1C). Consistent with this observation, energy dispersive spectroscopy (EDS) shows that the metal elements distribute uniformly throughout the films down to the ~1 nm level, without any indication of surface or grain boundary segregation (Fig. 1D, fig. S1).

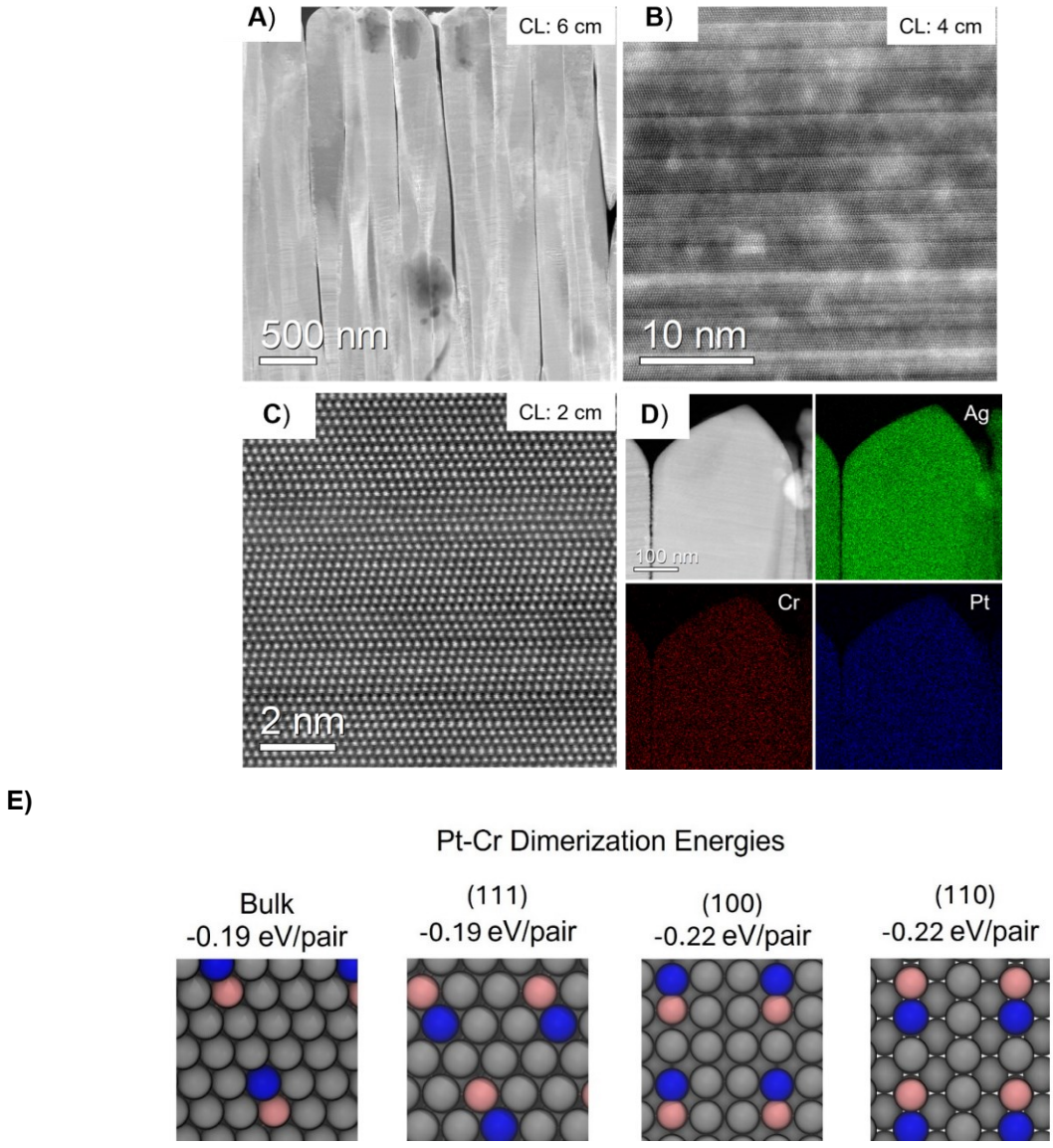

Figure 1. A) Low-magnification HAADF-STEM image of a Pt-Cr-Ag(10:10:80%) film grown on a poly-Ag substrate. High-magnification images of columnar grain at camera lengths (CL) of B) CL: 4 cm, C) CL: 2 cm. D) Elemental distribution map of Ag, Cr and Pt. E) Models of Pt-Cr pairs in bulk Ag and the (111), (100) and (110) surfaces and the Pt-Cr dimerization energies computed using DFT.

DFT predicts that Pt and Cr atoms substituted into Ag in low concentrations preferentially pair with one another to form stable heterometallic dimers. Pt-Cr dimerization is favorable by about 0.20 eV per pair within both the bulk and the dominant low-index surfaces of Ag (Fig. 1E), where the dimerization energy is defined relative to the dispersed state in which Pt and Cr atoms bond only with Ag atoms. The Pt-Cr

dimerization energy is high enough to stabilize the Pt-Cr pairs but likely low enough to avoid aggregation into large Pt-Cr rich domains. Consistent with this, calculations using DFT-derived energies for homo- and heterodimer formation indicate that Pt-Cr pairing is thermodynamically preferred for these materials even at reaction temperatures (see fig. S2). These DFT results thus suggest that Pt-Cr pairs will preferentially form and disperse throughout Ag, and that the dimerization energy should stabilize the Pt-Cr pairings within the bulk and the surfaces, thus suppressing adsorbate-driven segregation of one or more alloy components during catalysis.

Results and Discussion

Catalytic activity

APXPS experiments show that trimetallic Pt-Cr-Ag thin films are catalytically active toward ethanol (EtOH), converting it to acetaldehyde and H_2 with high selectivity. Fig. 2A shows image plots of gas-phase and surface C 1s spectra acquired every 14 seconds as a 10:10:80% Pt-Cr-Ag thin film was heated in 1 mbar of flowing EtOH. The gas-phase C 1s spectra show that the C 1s peaks from EtOH diminish while a C 1s peak from the carbonyl group of acetaldehyde simultaneously intensifies as the Pt-Cr-Ag film is first heated to 350 °C, reaching about 5% of the EtOH peak intensity, with these changes reversing as the film is cooled to the initial temperature. Mass spectrometry confirms that acetaldehyde and H_2 are the only species produced from EtOH during these experiments (fig. S3). The onset of catalytic activity occurs near 200 °C, and the reaction rate increases steadily and stabilizes as the sample temperature is increased and held at 350 °C. The surface C 1s spectra show that the coverage of EtOH-derived surface species (~285-287 eV) decreases as the Pt-Cr-Ag film becomes catalytically active during heating, and increases as the sample is cooled and its catalytic activity decreases (Fig. 2A, fig. S4). The oxygen coverage on the Pt-Cr-Ag film also decreases during catalytic ignition and is reversible (fig. S4). The gas-phase C 1s spectra shift toward higher apparent binding energy as the rate of EtOH dehydrogenation increases, indicating that the surface work function decreases [32] as the surface coverage of EtOH-derived species decreases. These results demonstrate that the Pt-Cr-Ag film is not only active and selective but also remains stable for periods of several hours while promoting highly selective catalytic dehydrogenation of EtOH.

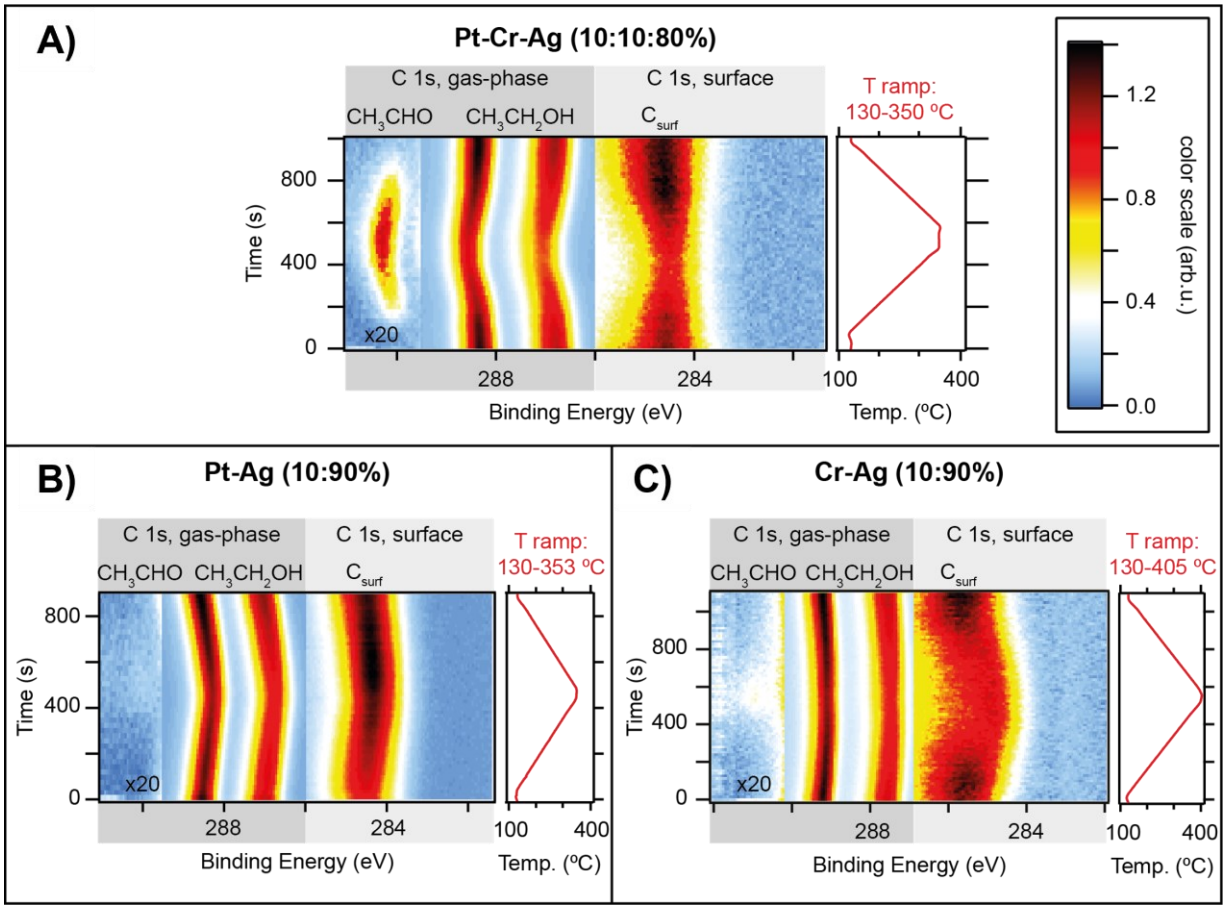

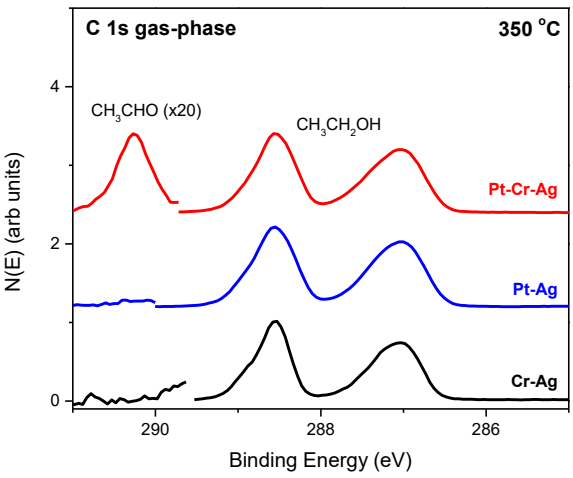

Figure 2. Trimetallic Pt-Cr-Ag films exhibit higher catalytic activity than bimetallic Pt-Ag and Cr-Ag films for selective EtOH dehydrogenation to acetaldehyde. Shown are image plots of XPS C 1s spectra of the gas-phase (left) and the surface (right) acquired as a function of time from alloy thin-films exposed to 1.0 mbar of EtOH while the samples were heated and cooled between 130 and ~350-405 °C (SM). Data are shown for thin films of A) Pt-Cr-Ag (10:10:80%), B) Pt-Ag (10:90%) and C) Cr-Ag (10:90%). Mass spectrometry (fig. S2) confirms the assignment of the C 1s peak near 291 eV to acetaldehyde (CH_3CHO). D) Comparison of C 1s gas-phase spectra acquired from the Pt-Cr-Ag, Pt-Ag and Cr-Ag films during reaction with EtOH at 350 °C.

In contrast to the trimetallic films, bimetallic (10:90%) Pt-Ag and Cr-Ag films exhibit negligible catalytic activity toward EtOH. For both bimetallic films, the gas-phase C 1s spectra reveal minimal EtOH consumption and a negligible signal from acetaldehyde during heating to 350 °C (Fig. 2B-D). For Pt-Ag, the C 1s spectra indicate carbon accumulation on the surface during heating in EtOH (Fig. 2B), whereas the oxygen coverage remains low (fig. S3). This behavior demonstrates that the Pt-Ag film promotes EtOH decomposition into carbonaceous surface species, but remains essentially inactive for catalyzing the conversion of EtOH to acetaldehyde or other gaseous products. Unlike Pt-Ag, carbon does not accumulate on the Cr-Ag film (Fig. 2C), but EtOH decomposition causes oxygen to accumulate instead (fig. S4), as elaborated below. The bimetallic Pt-Ag and Cr-Ag films thus have negligible activity for the catalytic conversion of EtOH compared with trimetallic Pt-Cr-Ag films (Fig. 2D), yet undergo restructuring due to EtOH decomposition.

The activity of trimetallic Pt-Cr-Ag films toward EtOH dehydrogenation and the much lower activity of the binary alloys is very reproducible and was also observed with a more dilute (x=0.05) $Pt_xCr_xAg_{1-2x}$ film (fig. S5). The differences in catalytic activity between the trimetallic and bimetallic alloys were also confirmed in separate measurements performed in a recirculating loop (batch) reactor (fig. S6). Our results thus demonstrate unequivocally that the trimetallic Pt-Cr-Ag surfaces are catalytically active in promoting the conversion of EtOH to acetaldehyde and H_2, whereas the binary Pt-Ag and Cr-Ag films are both nearly inactive.

Local coordination environments from bulk EXAFS

Ex-situ extended X-ray absorption fine structure (EXAFS) data, collected at the absorption edges of all constituent elements, demonstrates that the trimetallic films have similar local compositional motifs in $Pt_xCr_xAg_{1-2x}$ for all Pt and Cr loadings (x=0.02, 0.05 and 0.1). X-ray absorption near-edge structure (XANES) spectra at the Ag K-edge show that the local structure of Ag in the Pt-Cr-Ag films is similar to that in Ag foil (fig. S7), consistent with the high concentration of Ag in the films. In contrast, the Pt L_3 and Cr K-edge XANES spectra differ significantly from those collected from pure Pt and Cr metal foils, and lack signatures of Pt and Cr oxidation (fig. S7). These results indicate that Pt and Cr are alloyed in all of the thin films, consistent with the uniform distribution confirmed by EDS mapping (Fig. 1E, fig. S1).

EXAFS analysis demonstrates that Pt-Cr pairing occurs within all of these trimetallic alloy films, with the local Pt-Cr pair probabilities exceeding values for random alloys (table S1, fig. S8). Here, the Pt-Cr pair probability is defined as the fraction of nearest neighbor sites of Pt that are occupied by Cr. The analysis shows that the total coordination number of the first shell is consistent with bulk values for all elements, thus providing further evidence that the metals are well-dispersed throughout the trimetallic films (table S2, S3). Significantly, our analysis confirms that the Pt-Ag and Cr-Ag pair probabilities are lower, while the Pt-Cr (and Cr-Pt) pair probabilities are greater than random alloy values for each of the thin films investigated. For example, the EXAFS analysis yields a Pt-Cr pair probability of 37 $\pm$ 13% for the x=0.1 $Pt_xCr_xAg_{1-2x}$ film, indicating that, on average, each Pt atom has between 3–6 Cr nearest neighbors (out of 12 total) in the bulk of the film, and 1–3 Cr nearest neighbors within the dominant low-index surface planes (table S4). In contrast, the Pt-Pt and Cr-Cr pair probabilities (~5%) are significantly lower than the random-alloy expectation of 10% for the x=0.1 $Pt_xCr_xAg_{1-2x}$ film (table S4). Combined with STEM evidence excluding clusters larger than 1 nm in size, all the EXAFS results demonstrate the presence of Pt-Cr pair-ensembles. The ensembles are distributed nearly uniformly throughout the Pt-Cr-Ag films, but the slightly reduced Pt-Ag and Cr-Ag pair probabilities relative to a random mixture suggest a subtle preference for Pt and Cr atoms to group together, favoring Pt-Cr bonding.

In situ surface-site sensitive EXAFS

To confirm that the local ordering found in bulk EXAFS measurements is preserved near the surface, where catalysis takes place, we performed Pt L_3-edge grazing incidence (GI) EXAFS measurements for bimetallic Pt-Ag and trimetallic Pt-Cr-Ag films, grown 100 nm thick on float glass substrates. These spectra, acquired at an incident angle below the threshold for total external reflection, provide information about Pt in the outermost few nanometers of the samples [33]. The GI-EXAFS measurements for Pt-Ag and Pt-Cr-Ag thin films exhibit clear differences attributable to Pt-Cr pairing in the trimetallic alloy (Fig. 3, fig. S9, S10).

While spectra acquired for the bimetallic alloy can be adequately fit using only a single Pt-Ag component, indicating a high dispersion of Pt in the silver matrix with little Pt-Pt association, those from the trimetallic alloy require an additional Pt-Cr component (Fig. 3, table S5). This finding demonstrates that Pt and Cr atoms directly bond with one another in the near-surface region of the trimetallic alloys, in good agreement with our ex-situ EXAFS results and as predicted by DFT.

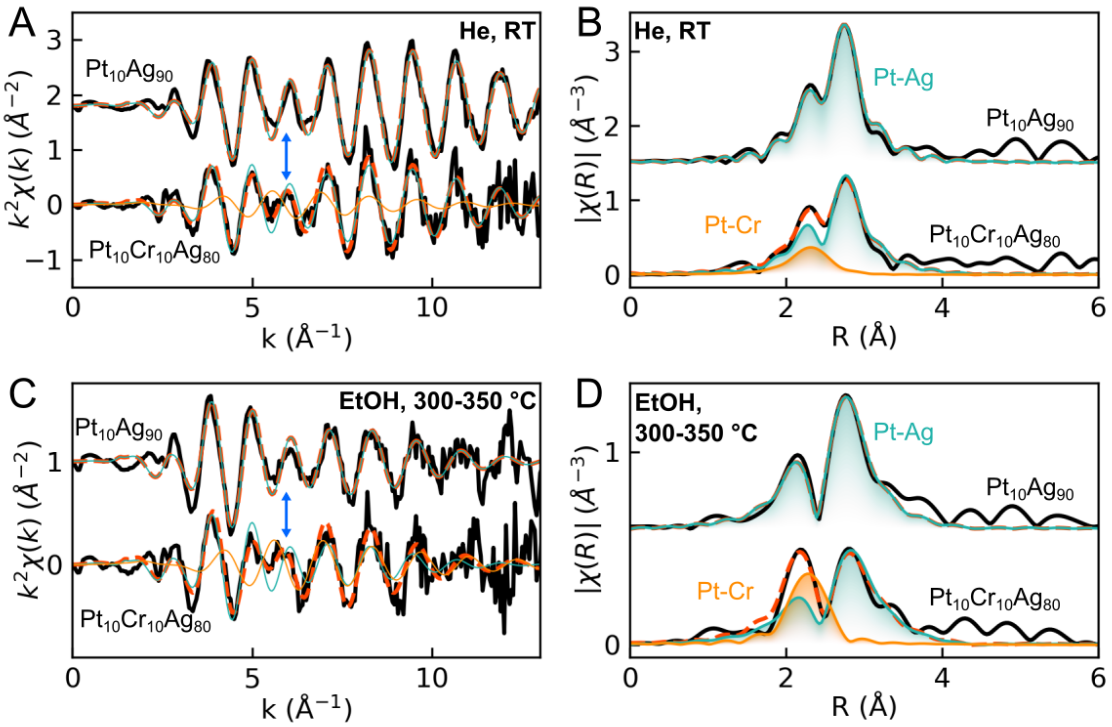

Figure 3. GI-EXAFS demonstrates that Pt and Cr atoms preferentially pair with one another in the near-surface region of Pt-Cr-Ag films. Reflectance Pt L_3-edge GI-EXAFS data (solid) and their fits (dashed) obtained from Pt-Ag (10:90%) and Pt-Cr-Ag (10:10:80%) films in A,B) helium at room temperature and C,D) EtOH at 300-350 °C. Scattering components for Pt-Ag (blue) and Pt-Cr (orange) are needed to accurately fit the data from the Pt-Cr-Ag film. The contribution of the Pt-Cr component is most apparent in the k-space plots (A,C) near k=6Å^{-1} due to an antiphase alignment with the Pt-Ag component (blue arrows).

The local structure of the Pt environment determined from Pt-L_3 edge GI-EXAFS data remained largely unchanged when the Pt-Cr-Ag film was heated from room temperature to 350 °C in helium or EtOH (Fig. 3, fig. S9, S10). The Pt-Cr pair probability determined from these experiments is 17 ± 6%, which is nearly double the Pt-Cr pair probability (10%) for random mixing in the trimetallic alloy (table S5). The GI-EXAFS results thus show that each Pt atom in the near-surface region has an average of 1 or 2 Cr nearest neighbors and importantly, that the Pt-Cr pairings remain stable under reaction conditions. Overall, both grazing incidence and bulk EXAFS demonstrate that Pt-Cr pairing occurs preferentially in the Pt-Cr-Ag thin films, and that this pairing is maintained close to the surface under reaction conditions, as required to influence catalytic behavior.

APXPS: Cr speciation and restructuring

APXPS, the most surface sensitive measurement used in this study, shows that both metallic and oxidized Cr were present on the Pt-Cr-Ag and Cr-Ag surfaces during exposure to EtOH, but that catalytic EtOH dehydrogenation only occurred on Pt-Cr-Ag due to the coexistence of metallic Cr and Pt. Deconvolution

of the Cr 2p + Ag $3p_{3/2}$ spectra shows that the Cr^{+3} oxidation state was the dominant form of Cr on both the Pt-Cr-Ag and Cr-Ag surfaces, and that both metallic Cr and Cr^{+6} were also present in smaller quantities (fig. S11). Although Cr_2O_3 was the majority state of Cr, our results demonstrate that oxidized Cr on the alloy surfaces was inactive toward EtOH dehydrogenation. For example, mass spectrometry shows that similar EtOH dehydrogenation activity was achieved on Pt-Cr-Ag surfaces on which the amount of surface Cr_2O_3 differed by more than a factor of two, but the amounts of metallic Cr were similar (fig. S12). Metallic Cr was also present on the Cr-Ag surface in similar or even higher concentrations compared with Pt-Cr-Ag (fig. S11c). However, given that the Cr-Ag film exhibited negligible catalytic activity toward EtOH dehydrogenation (Fig. 2C), our results indicate that metallic Cr in the form present on the Cr-Ag surface is also inactive toward the catalytic dehydrogenation of EtOH. Together, these findings demonstrate that catalytic EtOH dehydrogenation on the Pt-Cr-Ag surfaces requires the coexistence of metallic Cr and Pt. Since EXAFS reveals preferential Pt-Cr pairing, the combined APXPS and EXAFS results provide strong evidence that Pt-Cr pair sites serve as the active sites for EtOH dehydrogenation over the Pt-Cr-Ag alloy catalysts.

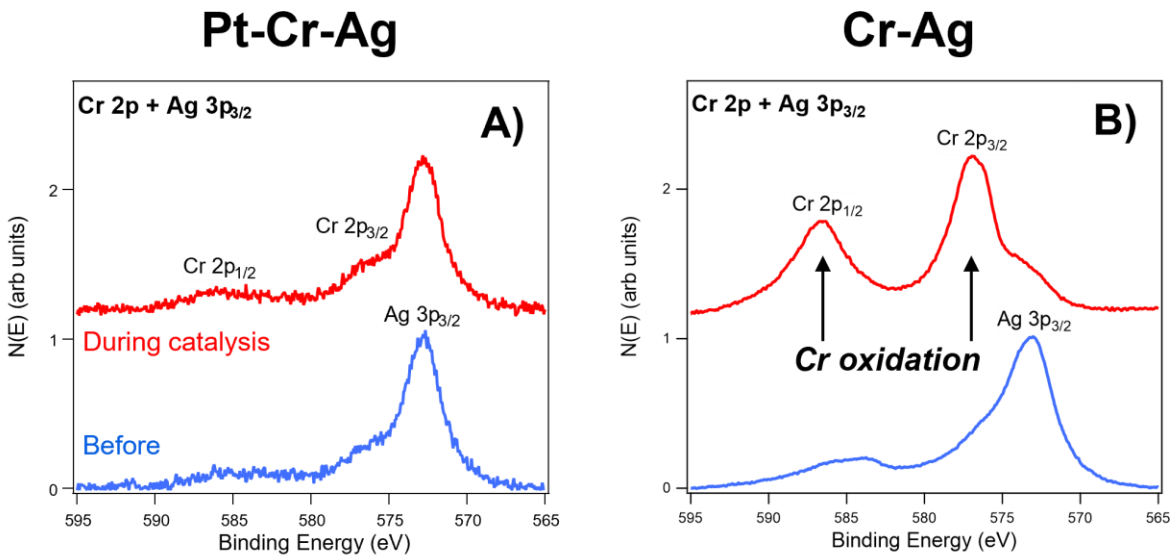

Figure 4. Pt stabilizes Cr on Pt-Cr-Ag surfaces during EtOH dehydrogenation, whereas EtOH deoxygenation induces Cr segregation and oxidation on Cr-Ag. Comparison of Cr 2p + Ag $3p_{3/2}$ spectra obtained from A) Pt-Cr-Ag and B) Cr-Ag films in vacuum at 130 °C and during exposure to EtOH at elevated temperature, after repeated heating-cooling between 130 and 350 or 400 °C. For the data shown, the Pt-Cr-Ag film was in 0.25 mbar EtOH and heated to 350 °C, and the Cr-Ag film was in 1.4 mbar EtOH and heated to 400 °C. Cr oxidation was also negligible on the Pt-Cr-Ag film at higher EtOH pressures up to 400 °C (fig. S11).

The Cr 2p spectra demonstrate that the Pt-Cr-Ag surfaces remain stable for prolonged durations during catalytic EtOH dehydrogenation, whereas the Cr-Ag surface undergoes significant restructuring due to deoxygenation of EtOH. For the trimetallic Pt-Cr-Ag films, the amount of Cr_2O_3 at the surface either remained constant (Fig. 4A) or slightly decreased (fig. S11a,b) when the films catalyzed the dehydrogenation of EtOH (0.25 to 1.25 mbar) at temperatures up to 400 °C, demonstrating that Cr_2O_3 was initially present on the Pt-Cr-Ag surfaces and not generated by EtOH. In sharp contrast, exposing the bimetallic Cr-Ag film to similar conditions caused Cr to oxidize to Cr_2O_3 (Fig. 4B, fig. S11c), with the surface Cr_2O_3 more than doubling from its initial amount, likely during the first thermal cycle. Analysis of the O 1s spectra shows that the surface oxygen coverage also more than doubled, primarily due to a more intense peak at 530.5 eV, consistent with lattice oxygen in Cr_2O_3 [34] (fig. S13). A smaller peak at 532 eV, attributed to OH and oxidized carbon species, also slightly intensified. Given the lack of C accumulation

on the Cr-Ag surface (Fig. 2C, fig. S4), we conclude that EtOH decomposition on the Cr-Ag thin film proceeds via deoxygenation, producing gaseous hydrocarbons while oxygen remains on the surface [20, 35]. The Cr_2O_3 phase was inactive toward EtOH up to 400 °C and its formation thus prevented sustained EtOH deoxygenation on the Cr-Ag surface. By comparison, no additional Cr oxidation occurs on the Pt-Cr-Ag surfaces, demonstrating that Pt-Cr pairing suppresses the ethanol-driven Cr oxidation and enables Pt-Cr sites to selectively catalyze EtOH dehydrogenation over extended periods. While the electronic origin requires further study, the Pt-Cr bonding interaction may prevent EtOH C-O bond activation by effectively lowering the oxophilicity of Cr, analogous to effects observed in electrochemical dealloying [36] and in other dilute alloys with early transition-metal dopants [35, 37].

APXPS: Pt speciation and coking

APXPS shows that Pt atoms on the Pt-Ag film become covered by carbonaceous species ("coke") due to non-selective EtOH decomposition, whereas negligible deactivation occurs on the Pt-Cr-Ag surfaces. For the Pt-Cr-Ag film, the overall intensity of the Pt $4f_{7/2}$ spectrum increased by about 50% after repeated cycles of EtOH dehydrogenation (Fig. 5A). A concurrent decrease in the carbon surface coverage (Fig. 5B, fig. S4) suggests that adsorbed C-species are removed from surface Pt sites during EtOH dehydrogenation on the Pt-Cr-Ag film, consistent with the conversion of Pt-bound intermediates to gaseous CH_3CHO. The C 1s surface spectra can be fit with two peaks for gaseous EtOH and three peaks at 287, 285.4 and 284.4 eV that are characteristic of oxidized carbon species, hydrocarbon species and atomic or graphitic C, respectively (fig. S14). The peaks at 287 and 285.4 eV diminished after repeated thermal cycling, indicating removal of oxidized and hydrocarbon species as the film became catalytically active, whereas the peak at 284.4 eV remained nearly constant, pointing toward the persistence of graphic (or atomic) carbon. Future studies using surface IR spectroscopy are likely to provide complementary insights into EtOH-derived surface species and reaction intermediates. A Pt $4f_{7/2}$ peak at 71.4 eV also emerged when the Pt-Cr-Ag film was catalytically active (Fig. 5A, fig. S15). DFT calculations suggest that this Pt $4f_{7/2}$ peak originates from Pt bonded to H-atoms (table S6), in agreement with the bifunctional mechanism predicted for EtOH dehydrogenation on Pt-Cr pairs in Ag(111) [20].

In contrast to the behavior of the Pt-Cr-Ag film, the total intensity of the Pt $4f_{7/2}$ signal from the Pt-Ag film decreased by approximately a factor of seven after repeated heating in EtOH to 400 °C (Fig. 5D). This loss of Pt 4f intensity was accompanied by a substantial increase in the graphitic (or atomic) carbon coverage, indicated by the C 1s peak at 284.4 eV (Fig. 5D, E, S14), while the oxygen coverage remained low (fig. S4). These results demonstrate that EtOH decomposition produces carbonaceous species that accumulate on Pt sites of the Pt-Ag film, leading to surface deactivation. Together, these findings demonstrate that preferential Pt-Cr pairing provides a "built-in" mechanism for stabilizing the active sites of Pt-Cr-Ag alloy surfaces to avoid coking and enable sustained catalytic EtOH dehydrogenation, and highlight the importance of *operando* spectroscopic measurements for characterizing dynamic changes in surface structure that occur under practical reaction conditions.

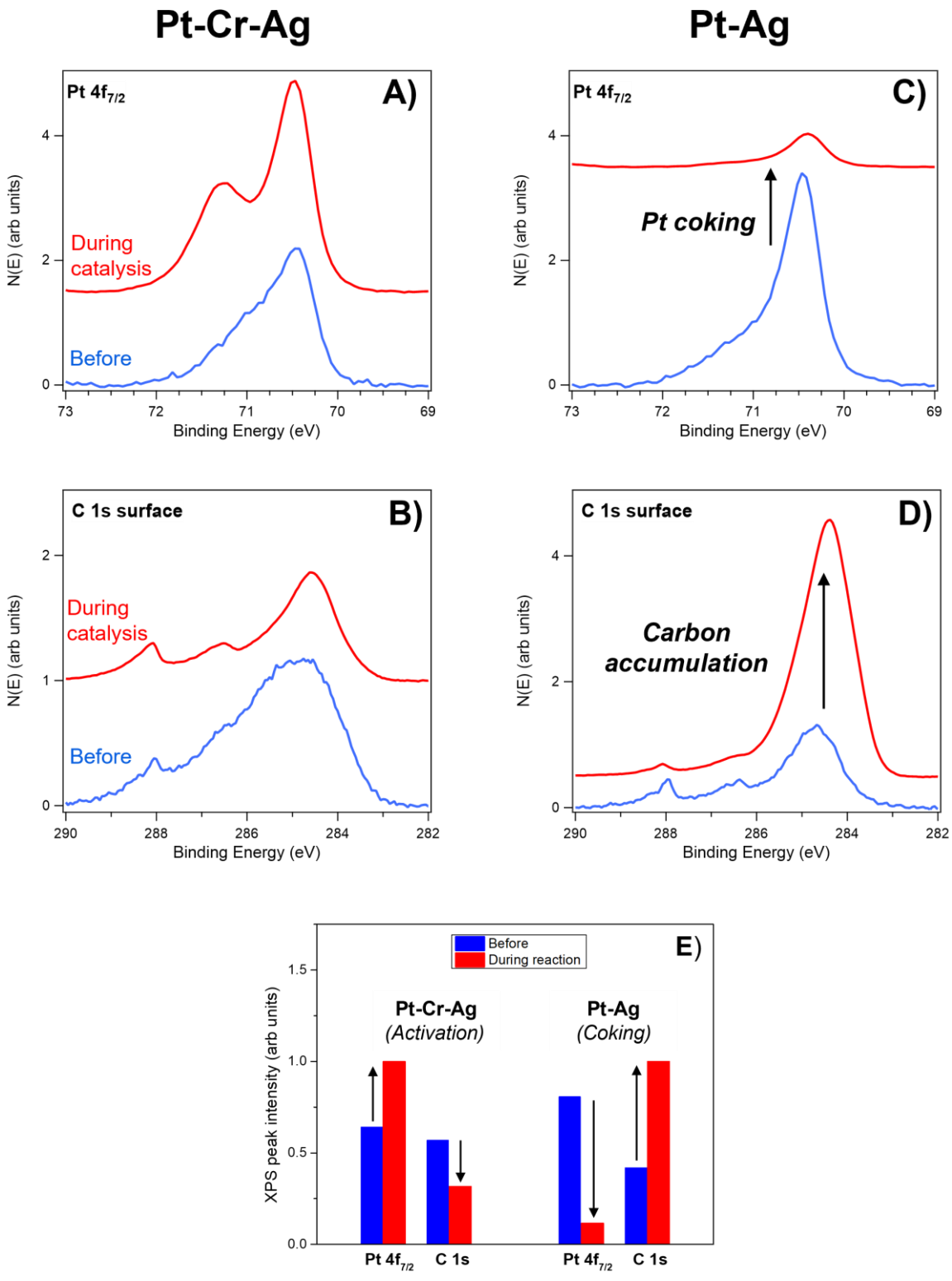

Figure 5. The Pt surface coverage remains high during EtOH dehydrogenation on the Pt-Cr-Ag surface, whereas EtOH decomposition causes carbon to accumulate on Pt sites of the Pt-Ag surface. Shown are APXPS Pt $4f_{7/2}$ and C 1s surface spectra obtained from a thin film of A, B) Pt-Cr-Ag (10:10:80%) and C ,D) Pt-Ag (10:90%) exposed to 1 mbar EtOH before (blue) and after (red) repeatedly heating to 350 or 400 °C. Attenuation of the Pt 4f signal from the Pt-Ag surface coincides with significant carbon accumulation as summarized in E).

Conclusions

The present study demonstrates that preferential Pt-Cr pairing in Pt-Cr-Ag alloys provides stable and selective sites for EtOH dehydrogenation while suppressing deactivation processes related to non-selective EtOH decomposition and surface segregation. The intrinsic stability of the Pt-Cr pair-sites enables Pt-Cr-Ag films with high loadings of the active metals to sustain their catalytic performance, demonstrating that trimetallic catalysts with heteropair ensembles can achieve higher activity than typical single-site catalysts while remaining selective and stable. Our findings also show that investigations with model crystalline surfaces [17, 20] can effectively identify trimetallic alloys that, when synthesized in polycrystalline form, achieve selective catalysis under practical operating conditions. As such, computational screening of the vast structure space of trimetallic systems may allow the efficient discovery of other heterometallic-pair trimetallic alloys for various applications in selective catalysis. Future efforts to stabilize heteropair sites in trimetallic nanoparticles will be critical for realizing the potential of these alloy catalysts in practical applications. Studies with model SAA surfaces have already enabled the development of several catalytic processes with high surface-area materials [38-42], suggesting that similar advances are achievable for trimetallic catalysts.

Supporting Information

The authors have cited additional references within the Supporting Information.

Acknowledgments

We thank the late Professor Robert J. Madix for his guidance and inspiration over the years. We thank Konstantin Klementiev and Mahesh Ramakrishnan for assistance with EXAFS measurements at Balder, and Weijia Wang, Robert Temperton and Andrey Shavorskiy for assistance with APXPS measurements at HIPPIE. We acknowledge Antonio Correa-Barrios and Jimmy Aut for performing the alloy depositions at LLNL. We thank S. Ehrlich, L. Ma and N. Marinkovic for help during synchrotron measurements at the QAS beamline.

This work was primarily supported as part of the Integrated Mesoscale Architectures for Sustainable Catalysis, an Energy Frontier Research Center funded by the U.S. Department of Energy, Office of Science, Basic Energy Sciences under Award No. DE-SC0012573. Electron microscopy was performed at the Singh Center for Nanotechnology, which is supported by the NSF National Nanotechnology Coordinated Infrastructure Program under grant NNCI-2025608. Additional support for the NSF through the University of Pennsylvania Materials Research Science and Engineering Center (MRSEC) (DMR-1720530; DMR-2309043). This research used beamline 7-BM (QAS) of the National Synchrotron Light Review Source II, a U.S. DOE Office of Science User Facility operated for the DOE Office of Science by Brookhaven National Laboratory under Contract No. DE-SC0012704. It used BL2-2 beamline of the Stanford Synchrotron Radiation Lightsource (SSRL) of the SLAC National Laboratory. Use of SSRL was supported by DOE under Contract No. DE-AC02-76SF00515. 7-BM beamline operations were supported in part by the Synchrotron Catalysis Consortium (U.S. DOE, Office of Basic Energy Sciences, Grant DE-SC0012335). We acknowledge the MAX IV Laboratory for time on the HIPPIE and Balder beamlines under proposals (20220980, 20221042). Research conducted at MAX IV, a Swedish national user facility, is supported by the Swedish Research council under contract 2018-07152, the Swedish Governmental Agency for Innovation Systems under contract 2018-04969, and Formas under contract 2019-02496. JFW also gratefully acknowledges the NSF for support under grant CBET-2323274 for analysis of APXPS data. MMM and ECHS thank the NSF under a collaborative grant (NSF CHE-2334969 and NSF CHE-2334970) for support for calculations and analysis. AIF acknowledges support of the NSF grant NSF CHE-2203858 for analysis of coordination numbers in multimetallic alloys. APXPS and EXAFS experiments at MAXIV and their analysis and interpretation were supported by the Swedish Research Council (U.K. 2022-04363, J.K. 2017-04840, 2022-04363, L.R.M. and H.W. 2018-05374, 2022-04828, J.Z. and L.R. 2023-04708). U.K. and J.K. also acknowledge financial support for APXPS experiments and analysis from the Crafoord

foundation. Recirculating reactor reactivity measurements were performed at the Center for Functional Nanomaterials, Brookhaven National Laboratory, supported by the U.S. Department of Energy, Office of Basic Energy Sciences, under Contract No. DE-SC0012704. Work at LLNL was performed under the auspices of the U.S. DOE by LLNL under Contract DE-AC52–07NA27344.

Keywords: operando spectroscopy • dual atom alloy • ethanol dehydrogenation • catalyst selectivity • catalyst stability

References

[1] R. T. Hannagan, G. Giannakakis, M. Flytzani-Stephanopoulos, E. C. H. Sykes, "Single-atom alloy catalysts", *Chem. Rev.* **2020**, *120*, 12044–12088.

[2] A. Q. Wang, J. Li, T. Zhang, "Heterogeneous single-atom catalysis", *Nat. Rev. Chem.* **2018**, *2*, 65-81.

[3] S. K. Kaiser, Z. P. Chen, D. F. Akl, S. Mitchell, J. Pérez-Ramírez, "Single-Atom Catalysts across the Periodic Table", *Chem. Rev.* **2020**, *120*, 11703-11809.

[4] J. P. Simonovis, A. Hunt, S. D. Senanayake, I. Waluyo, "Subtle and reversible interactions of ambient pressure H_2 with Pt/Cu(111) single-atom alloy surfaces", *Surf. Sci.* **2019**, *679*, 207-213.

[5] A. J. Mccue, J. A. Anderson, "CO induced surface segregation as a means of improving surface composition and enhancing performance of CuPd bimetallic catalysts", *J. Catal.* **2015**, *329*, 538-546.

[6] K. R. Yang, B. Yang, "Surface restructuring of Cu-based single-atom alloy catalysts under reaction conditions: the essential role of adsorbates", *Phys. Chem. Chem. Phys.* **2017**, *19*, 18010-18017.

[7] Q. Fu, Y. Luo, "Catalytic Activity of Single Transition-Metal Atom Doped in Cu(111) Surface for Heterogeneous Hydrogenation", *J. Phys. Chem. C* **2013**, *117*, 14618-14624.

[8] K. G. Papanikolaou, M. T. Darby, M. Stamatakis, "CO-Induced Aggregation and Segregation of Highly Dilute Alloys: A Density Functional Theory Study", *J. Phys. Chem. C* **2019**, *123*, 9128-9138.

[9] M. Ouyang, K. G. Papanikolaou, A. Boubnov, A. S. Hoffman, G. Giannakakis, S. R. Bare, M. Stamatakis, M. Flytzani-Stephanopoulos, E. C. H. Sykes, "Directing reaction pathways via in situ control of active site geometries in PdAu single-atom alloy catalysts", *Nat. Commun.* **2021**, *12*, 1549.

[10] N. Marcella, J. S. Lim, A. M. Plonka, G. Yan, C. J. Owen, J. E. S. van der Hoeven, A. C. Foucher, H. T. Ngan, S. B. Torrisi, N. S. Marinkovic, E. A. Stach, J. F. Weaver, J. Aizenberg, P. Sautet, B. Kozinsky, A. I. Frenkel, "Decoding reactive structures in dilute alloy catalysts", *Nat. Commun.* **2022**, *13*, 832.

[11] T. W. He, A. R. P. Santiago, Y. C. Kong, M. A. Ahsan, R. Luque, A. J. Du, H. Pan, "Atomically Dispersed Heteronuclear Dual-Atom Catalysts: A New Rising Star in Atomic Catalysis", *Small* **2022**, *18*, 2106091.

[12] E. J. Guan, J. Ciston, S. R. Bare, R. C. Runnebaum, A. Katz, A. Kulkarni, C. X. Kronawitter, B. C. Gates, "Supported Metal Pair-Site Catalysts", *ACS Catal.* **2020**, *10*, 9065-9085.

[13] D. Kiani, I. E. Wachs, "The Conundrum of "Pair Sites" in Langmuir-Hinshelwood Reaction Kinetics in Heterogeneous Catalysis", *ACS Catal.* **2024**, *14*, 10260-10270.

[14] Y. R. Ying, X. Luo, J. L. Qiao, H. T. Huang, ""More is Different:" Synergistic Effect and Structural Engineering in Double-Atom Catalysts", *Adv. Funct. Mater.* **2021**, *31*, 2007423.

[15] D. Zhao, Z. W. Zhuang, X. Cao, C. Zhang, Q. Peng, C. Chen, Y. D. Li, "Atomic site electrocatalysts for water splitting, oxygen reduction and selective oxidation", *Chem. Soc. Rev.* **2020**, *49*, 2215-2264.

[16] M. K. Samantaray, R. Dey, S. Kavitake, E. Abou-Hamad, A. Bendjeriou-Sedjerari, A. Hamieh, J. M. Basset, "Synergy between Two Metal Catalysts: A Highly Active Silica-Supported Bimetallic W/Zr Catalyst for Metathesis of n-Decane", *J. Am. Chem. Soc.* **2016**, *138*, 8595-8602.

[17] S. J. Zhang, E. C. H. Sykes, M. M. Montemore, "Tuning reactivity in trimetallic dual-atom alloys: molecular-like electronic states and ensemble effects", *Chem. Sci.* **2022**, *13*, 14070-14079.

[18] A. Dasgupta, R. M. Rioux, "Intermetallics in catalysis: An exciting subset of multimetallic catalysts", *Catal. Today* **2019**, *330*, 2-15.

[19] M. Armbruster, R. Schlogl, Y. Grin, "Intermetallic compounds in heterogeneous catalysis-a quickly developing field", *STAM* **2014**, *15*, 034803.

[20] P. L. Kress, S. J. Zhang, Y. C. Wang, V. Cinar, C. M. Friend, E. C. H. Sykes, M. M. Montemore, "A Priori Design of Dual-Atom Alloy Sites and Experimental Demonstration of Ethanol Dehydrogenation and Dehydration on PtCrAg", *J. Am. Chem. Soc.* **2023**, *145*, 8401-8407.

[21] G. O. Kayode, M. M. Montemore, "Factors controlling oxophilicity and carbophilicity of transition metals and main group metals", *J. Mater. Chem. A* **2021**, *9*, 22325-22333.
[22] J. F. Pang, M. Yin, P. F. Wu, X. Q. Li, H. Y. Li, M. Y. Zheng, T. Zhang, "Advances in catalytic dehydrogenation of ethanol to acetaldehyde", *Green Chem.* **2021**, *23*, 7902-7916.
[23] D. Behrendt, S. Banerjee, C. Clark, A. M. Rappe, "High-Throughput Computational Screening of Bioinspired Dual-Atom Alloys for CO2 Activation", *J. Am. Chem. Soc.* **2023**.
[24] Y. Y. Wang, C. M. Tang, Q. L. Li, T. Xiao, F. J. Xiong, "Theoretical prediction of efficient Cu-based dual-atom alloy catalysts for electrocatalytic nitrate reduction to ammonia high-throughput first-principles calculations", *J. Mater. Chem. A* **2025**, *13*, 3765-3776.
[25] A. Das, D. Roy, S. Manna, B. Pathak, "Harnessing the Potential of Machine Learning to Optimize the Activity of Cu-Based Dual Atom Catalysts for CO_2 Reduction Reaction", *Acs Materials Letters* **2024**, *6*, 5316-5324.
[26] X. Guan, W. Gao, M. L. Xiao, C. P. Liu, W. Xing, "Theoretical predictions of high-performance dual-atom alloys for the decomposition of formic acid", *Materials Today Sustainability* **2024**, *27*.
[27] C. A. Zhou, J. Y. Zhao, P. F. Liu, J. F. Chen, S. Dai, H. G. Yang, P. Hu, H. F. Wang, "Towards the object-oriented design of active hydrogen evolution catalysts on single-atom alloys", *Chem. Sci.* **2021**, *12*, 10634-10642.
[28] K. Chen, D. Y. Ma, Y. Zhang, F. Z. Wang, X. Yang, X. M. Wang, H. Zhang, X. J. Liu, R. Bao, K. Chu, "Urea Electrosynthesis from Nitrate and CO_2 on Diatomic Alloys", *Adv. Mater.* **2024**, *36*.
[29] R. Zhang, J. Y. Chen, Y. H. Huang, J. A. Tang, R. X. Zhao, Y. X. Liu, L. Lei, D. G. Wang, L. Li, Z. Liu, "One-Step Laser Synthesis of Dual-Atom Alloy Catalysts for Hydrogen Evolution Reaction", *Adv. Funct. Mater.* **2025**, *35*.
[30] S. J. Pennycook, & Nellist, P. D., "Scanning transmission electron microscopy: imaging and analysis", Springer Science & Business Media, **2011**.
[31] P. J. Phillips, M. C. Brandes, M. J. Mills, M. De Graef, "Diffraction contrast STEM of dislocations: Imaging and simulations", *Ultramicroscopy* **2011**, *111*, 1483-1487.
[32] S. Axnanda, M. Scheele, E. Crumlin, B. H. Mao, R. Chang, S. Rani, M. Faiz, S. D. Wang, A. P. Alivisatos, Z. Liu, "Direct Work Function Measurement by Gas Phase Photoelectron Spectroscopy and Its Application on PbS Nanoparticles", *Nano Lett.* **2013**, *13*, 6176-6182.
[33] S. M. Heald, H. Chen, J. M. Tranquada, "Glancing-Angle Extended X-Ray-Absorption Fine-Structure and Reflectivity Studies of Interfacial Regions", *Phys. Rev. B* **1988**, *38*, 1016-1026.
[34] B. P. Payne, M. C. Biesinger, N. S. McIntyre, "X-ray photoelectron spectroscopy studies of reactions on chromium metal and chromium oxide surfaces", *J. Electron. Spectrosc. Relat. Phenom.* **2011**, *184*, 29-37.
[35] J. J. Shi, H. T. Ngan, P. Sautet, J. F. Weaver, "High Selectivity and Activity of Ti-Cu(111) Dilute Alloys for the Deoxygenation of Ethanol to Ethylene", *ACS Catal.* **2023**, *13*, 11244-11255.
[36] K. Sieradzki, N. Dimitrov, D. Movrin, C. McCall, N. Vasiljevic, J. Erlebacher, "The dealloying critical potential", *J. Electrochem. Soc.* **2002**, *149*, B370-B377.
[37] A. J. R. Hensley, Y. C. Hong, R. Q. Zhang, H. Zhang, J. M. Sun, Y. Wang, J. S. McEwen, "Enhanced Fe2O3 Reducibility via Surface Modification with Pd: Characterizing the Synergy within Pd/Fe Catalysts for Hydrodeoxygenation Reactions", *ACS Catal.* **2014**, *4*, 3381-3392.
[38] A. Jalil, E. E. Happel, L. Cramer, A. Hunt, A. S. Hoffman, I. Waluyo, M. M. Montemore, P. Christopher, E. C. H. Sykes, "Nickel promotes selective ethylene epoxidation on silver", *Science* **2025**, *387*, 869-873.
[39] R. T. Hannagan, G. Giannakakis, R. Réocreux, J. Schumann, J. Finzel, Y. C. Wang, A. Michaelides, P. Deshlahra, P. Christopher, M. Flytzani-Stephanopoulos, M. Stamatakis, E. C. H. Sykes, "First-principles design of a single-atom-alloy propane dehydrogenation catalyst", *Science* **2021**, *372*, 1444-1447.
[40] M. D. Marcinkowski, M. T. Darby, J. L. Liu, J. M. Wimble, F. R. Lucci, S. Lee, A. Michaelides, M. Flytzani-Stephanopoulos, M. Stamatakis, E. C. H. Sykes, "Pt/Cu single-atom alloys as coke-resistant catalysts for efficient C-H activation", *Nature Chem.* **2018**, *10*, 325-332.
[41] F. R. Lucci, J. L. Liu, M. D. Marcinkowski, M. Yang, L. F. Allard, M. Flytzani-Stephanopoulos, E. C. H. Sykes, "Selective hydrogenation of 1,3-butadiene on platinum-copper alloys at the single-atom limit", *Nat. Commun.* **2015**, *6*, 8550.
[42] J. J. Shan, F. R. Lucci, J. L. Liu, M. El-Soda, M. D. Marcinkowski, L. F. Allard, E. C. H. Sykes, M. Flytzani-Stephanopoulos, "Water co-catalyzed selective dehydrogenation of methanol to formaldehyde and hydrogen", *Surf. Sci.* **2016**, *650*, 121-129.

Entry for Table of Contents

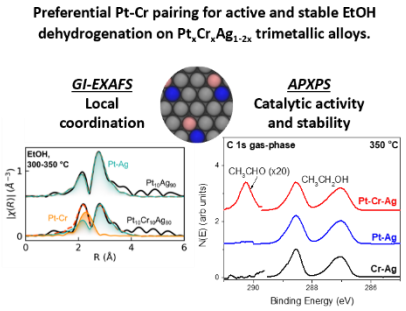

Trimetallic $Pt_xCr_xAg_{1-x}$ ($x < 0.1$) alloys feature active Pt-Cr pairs for non-oxidative ethanol dehydrogenation. Operando X-ray spectroscopy confirms the preferential formation of Pt-Cr pairs dispersed throughout an Ag matrix and demonstrates that the Pt-Cr sites have high activity and selectivity for catalytic ethanol dehydrogenation, while suppressing reactions that deactivate binary Pt-Ag and Cr-Ag alloys.